19th Brazilian Congress of Thermal Sciences and Engineering
November 6th–10th, 2022, Bento Gonçalves - RS - Brazil

ENC-2022-0013
NUMERICAL SIMULATION OF FLOWS IN CONJUGATED REGIONS USING THE FINITE ELEMENT METHOD TO SOLVE THE DARCY-FORCHHEIMER MOMENTUM AND ENERGY EQUATIONS

João P. I. Souza
Gustavo R. Anjos
Universidade Federal do Rio de Janeiro
jpisouza@mecanica.coppe.ufrj.br
gustavo.rabello@coppe.ufrj.br

Abstract. *Fluid dynamics with heat transfer problems have complex modeling equations to be solved analytically. Thus, numerical methods, such as the Finite Element Method (FEM), are broadly used in order to simulate such phenomena for any geometry. The current study aims at simulating flows in conjugated regions, where free-flow and porous regions are present. The mathematical modeling is made through mass and momentum equations discretized by the Finite Element Method (FEM) along with the semi-lagrangian technique, where unconditional stability is successfully achieved for the numerical solution in different geometries. The Darcy-Forcheimer term is included in the classical Navier-Stokes equation, so that the resistance imposed by the porous medium is considered in the pressure gradient. The quadratic triangle mesh element fulfil the well-known LBB condition, assuring stability and 2nd order convergence, when compared to simpler kinds of elements. Additionally, a mesh convergence is made by comparing results with the literature for meshes with different sizes. As to the temperature, an analysis on how the porous medium interferes in the convective heat transfer is provided, showing that, in conjugated flows, heat transfer is significantly different from one region to the other, due to the effects of the porous medium on convection. A pure convective case is also shown, in order to demonstrate how temperature gradient, associated with a gravitational field can induce convective streamlines in a confined region. The code is written in Python in an optimized object-oriented programming, so that refined meshes are easily used to simulate these phenomena, providing more accurate results as the more elements are used. Also, an optimized method for the semi-lagrangian was implemented, reducing simulation time.*

Keywords: *CFD, FEA, Conjugated Flow, Darcy/Forchheimer*

1. INTRODUCTION

It is widely known, among the scientific mechanical engineering community, that, when it comes to fluid mechanics or flow studies, the Navier-Stokes equations are an important and crucial point to be studied, along with the continuity equation, as presented by Batchelor (2000). As can be noticed, this set of equations, in spite of being a powerful way of characterizing the behavior of any sort of flow, has a complex form, mainly due to its non-linearity, with respect to velocity variables. Therefore, the analytical solution for them, as well as for some problems of heat conduction "can only be obtained in some simplified cases" Zhang *et al.* (2018). Given that most common cases may not be simplified without considerable loss of information and representativeness of the phenomenon, numerical solutions are required.

Analyzing different methods to solve said system of equations, it is important to discuss a few of them. Bessaih *et al.* (2018) proposed a technique for the three-dimensional Navier-Stokes system of equations, which is notably more complex than the two dimensional one, and must be solved for some detailed cases, where the two-dimensional approach will not satisfy all the requisites. This technique consists in introducing a delay in the non-linear term ($\mathbf{u} \cdot \nabla \mathbf{u}$), which, according to Bessaih *et al.* (2018), "introduces a regularizing effect in the equations and allows to prove the uniqueness of weak solutions". Abdelwahed *et al.* (2011) analyze the two-dimensional form of the Navier-Stokes equations and proposes the use of the finite element method to find a solution for them. For that, Abdelwahed *et al.* (2011) use the stream function (ψ) and vorticity (ω) in the z direction formulation, modifying the set of equations to the vorticity form. Toro *et al.* (2018) also make use of the finite element technique, providing examples on both flow and heat transfer phenomena. In this case, instead of using stream function vorticity, the authors simulate a potential flow, therefore an ideal fluid, around a cylinder.

Alternatively, Bagai *et al.* (2020) use the stream function-vorticity approach as well but, instead of the finite element

method for the numerical solution, the authors use the finite difference approximation for the derivatives. The problem examined to validate the method is the four-sided lid driven cavity, with heat and mass transfer coupled to the fluid mechanics problem. The same method is also used by Zitouni *et al.* (2020) in a TIG welding, where both thermal and fluid flow phenomena are modeled, evidentiating how broad flow simulation can be.

For porous region analysis, the work seen in Cimolin and Discacciati (2013) is used as reference for the Darcy/ Forchheimer formulation. The authors describe three different models to describe a mixed region (porous and free) problem. The first one is the Navier-Stokes/Darcy (NSD) model, the Navier–Stokes/Forchheimer (NSF) model and the Penalization (PE) model. For the first two, the formulation is uncoupled, having the interface connected by boundary conditions. As for the PE model, the whole domain is described with a single equation of momentum conservation, which simplifies the solver. As stated by the authors, the PE method is a good approximation of the physical problem, in spite of interface being more well represented by the first two. This current work will be based on the PE method, since the interface is of low interest for the purpose of this thesis. A similar approach is also used by Mesquida (2019), who makes use of a CFD software to simulate a gasoline particle filter, using the Reynolds Average Numerical solution, also referred to as RANS, approach for turbulent regimes.

Thus, for this work, the main objective is to propose an integrated solution for conjugated flows with heat transfer using the finite element method in the Darcy/Forchheimer formulation. This solution uses the penalization model (PE) proposed by Cimolin and Discacciati (2013) as a way of coupling both free-flow and porous domains in one single set of differential equations.

2. GOVERNING EQUATIONS

The governing equation for an incompressible fluid phase in its vectorial form is given by equation 1, known as the Navier-Stokes equation, as presented by Batchelor (2000).

$$\frac{\partial \mathbf{u}}{\partial t} + \mathbf{u} \cdot \nabla \mathbf{u} - \nu \nabla^2 \mathbf{u} + \frac{1}{\rho} \nabla p = \mathbf{g} \tag{1}$$

Here, $\mathbf{u}$ is the velocity vector, p the pressure and ν the kinematic viscosity. g is a field source term, generally representing gravitational field. The non-dimensional variables for cases where a characteristic velocity U is identified, such as an expansion, are calculated as follows, where the subscript D indicates the dimensional variable:

$$\mathbf{x} = \frac{\mathbf{x}_D}{L}, \quad \mathbf{u} = \frac{\mathbf{u}_D}{U}, \quad t = \frac{t_D U}{L}, \quad \mathbf{g} = \frac{\mathbf{g}_D}{|\mathbf{g}_{ref}|}, \quad p = \frac{p_D}{\rho U^2} \tag{2}$$

Replacing the dimensional values by correlations (2), one may find the continuity (Eq. 3) and the momentum equation for porous media (Eq. 4), known as Darcy/Forchheimer equation, in non-dimensional forms. Eq. 5 is the energy equation, that can be solved to find the temperature field.

$$\nabla \cdot \mathbf{u} = 0 \tag{3}$$

$$\frac{D\mathbf{u}}{Dt} + \frac{\varphi}{ReDa} \left(\mathbf{u} + Fo\varphi |\mathbf{u}| \mathbf{u} \right) \varepsilon = -\nabla p + \frac{1}{Re} \nabla^2 \mathbf{u} + \frac{1}{Fr^2} \mathbf{g} \tag{4}$$

$$\frac{\partial T}{\partial t} + \mathbf{u} \cdot \nabla T = \frac{1}{RePr} \left(\nabla^2 T \right) \tag{5}$$

φ is the porosity of the medium and ε defines if the region is either porous, assuming the value of 1, or not, with a null value. $Re = UL/\nu$ is known as the Reynolds number, $Pr = \nu/\alpha$ is the Prandtl number, where α is the thermal diffusivity, $Da = K/L^2$ is the Darcy number, $Fo = \rho C_F \sqrt{K} U/\mu$ the Forchheimer number and $Fr = U/\sqrt{gL}$ the Froude number.

3. THE FINITE ELEMENT METHOD

In this section, the variational and the discrete forms will be shown for the Navier-Stokes equation and, then, the Darcy/Forchheimer terms will be added to the final linear system of equations.

3.1 The Variational Form

According to Zienkiewicz and Taylor (2000), the weak form, also known as variational form, is obtained by multiplying each of the governing equation by the weight functions w, q and r, associated with velocity, pressure and temperature, respectively. The Green theorem is applied to the second order and pressure gradient terms. Since, in this work, all boundary conditions are either Dirichlet or null Neumann, the boundary integral resulted from such theorem is null and the final variational form is given by:

$$\int_\Omega \frac{D\mathbf{u}}{Dt}\cdot\mathbf{w}d\Omega + \int_\Omega \frac{\varphi\varepsilon}{ReDa}\left(\mathbf{u}+Fo\varphi|\mathbf{u}|\mathbf{u}\right)\cdot\mathbf{w}d\Omega = \int_\Omega p\nabla\cdot\mathbf{w}d\Omega - \frac{1}{Re}\int_\Omega\left(\nabla\mathbf{u}:\nabla\mathbf{w}\right)d\Omega + \int_\Omega\frac{1}{Fr^2}\mathbf{g}\cdot\mathbf{w}d\Omega \quad (6)$$

$$\int_\Omega \frac{du}{dx}wd\Omega + \int_\Omega \frac{dv}{dy}wd\Omega = 0 \quad (7)$$

$$\int_\Omega \frac{DT}{Dt}wd\Omega = -\frac{1}{RePr}\int_\Omega\left(\nabla T\cdot\nabla w\right)d\Omega \quad (8)$$

3.2 The Galerkin Method

The Galerkin Method consists of an approximation of the continuous variable to a discrete representation. Then, the shape functions N are used, in order to interpolate the values in the nodes seen in Figure 1.

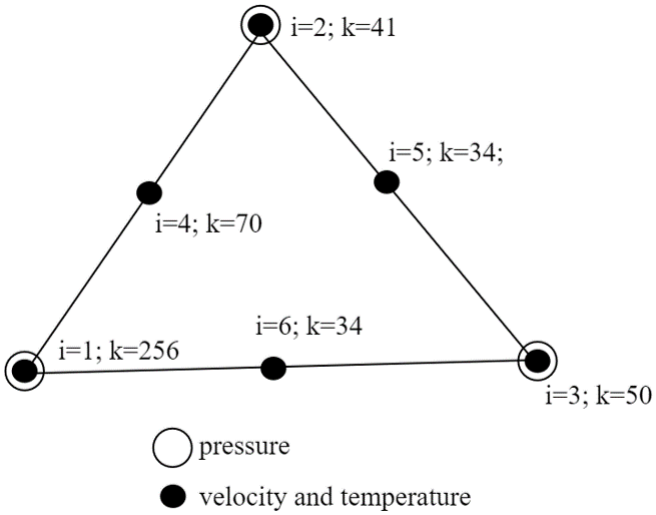

Figure 1: Element's nodes representation, with local (i) and respective global (k) numbers, for quadratic elements.

Given the elements, the entire mesh is composed by a set of triangular elements, with a total of NP_{total} points, for which the velocities u and v and the temperature are calculated, and NV_{total} vertices, where pressure is associated. The element shown satisfies the LBB condition and the difference between NV and NP is that NV does not account for the midpoints, seen in Figure 1. The variables of interest and their respectful weight functions $\mathbf{w}$, q and r are presented next:

$$u\approx\sum_{i=1}^{NP}N_i(x,y)u_i,\quad v\approx\sum_{i=1}^{NP}N_i(x,y)v_i,\quad p\approx\sum_{i=1}^{NV}L_i(x,y)p_i,\quad T\approx\sum_{i=1}^{NP}N_i(x,y)T_i \quad (9)$$

$$\mathbf{w} \approx \sum_{j=1}^{NP} N_j(x,y)\mathbf{w}_j, \quad q \approx \sum_{j=1}^{NV} L_j(x,y)q_j, \quad r \approx \sum_{j=1}^{NV} N_j(x,y)r_j \tag{10}$$

Substituting the approximated variables, as well as the weight approximated forms, into the governing equations and using the index notation leads to:

$$\sum_e \int_{\Omega_e} \frac{DN_i u_i}{Dt} N_j w_{x_j} d\Omega + \frac{1}{ReDa} \sum_e \int_{\Omega_e} \varphi_e \varepsilon_e (N_i u_i + \varphi Fo |\mathbf{u}|_i N_i u_i) N_j w_{x_j} d\Omega - \sum_e \int_{\Omega_e} \frac{\partial N_i w_{x_i}}{\partial x} L_j p_j d\Omega + \frac{1}{Re} \sum_e \int_{\Omega_e} \left(\nabla N_i u_i \cdot \nabla N_j w_{x_j} \right) d\Omega - \sum_e \int_{\Omega_e} \frac{1}{Fr^2} N_i g_{x_i} N_j w_{x_j} d\Omega = 0 \tag{11}$$

$$\sum_e \int_{\Omega_e} \frac{DN_i v_i}{Dt} N_j w_{y_j} d\Omega + \frac{1}{ReDa} \sum_e \int_{\Omega_e} \varphi_e \varepsilon_e (N_i v_i + \varphi Fo |\mathbf{u}|_i N_i v_i) N_j w_{y_j} d\Omega - \sum_e \int_{\Omega_e} \frac{\partial N_i w_{y_i}}{\partial y} L_j p_j d\Omega + \frac{1}{Re} \sum_e \int_{\Omega_e} \left(\nabla N_i v_i \cdot \nabla N_j w_{y_j} \right) d\Omega - \sum_e \int_{\Omega_e} \frac{1}{Fr^2} N_i g_{y_i} N_j w_{y_j} d\Omega = 0 \tag{12}$$

$$\sum_e \left(\int_{\Omega_e} L_i q_i \frac{\partial N_j u_j}{\partial x} d\Omega + \int_{\Omega_e} L_i q_i \frac{\partial N_j v_j}{\partial y} d\Omega \right) = 0 \tag{13}$$

$$\sum_e \left(\int_{\Omega_e} \frac{DN_i T_i}{Dt} N_j r_j d\Omega + \frac{1}{RePr} \int_{\Omega_e} \left(\nabla N_i T_i \cdot \nabla N_j r_j \right) d\Omega \right) = 0 \tag{14}$$

Since w_j appears on both sides of all the equations, it may be eliminated. Grouping and rearranging the terms, the matrices of the linear systems are presented as follows.

$$M_{ij} = \sum_e \left(\int_{\Omega_e} N_i N_j d\Omega \right), \quad K_{ij} = \sum_e \left(\int_{\Omega_e} \nabla N_i \cdot \nabla N_j d\Omega \right) \tag{15}$$

$$G_{x_{ij}} = \sum_e \left(\int_{\Omega_e} \frac{\partial N_i}{\partial x} L_j d\Omega \right), \quad G_{y_{ij}} = \sum_e \left(\int_{\Omega_e} \frac{\partial N_i}{\partial y} L_j d\Omega \right) \tag{16}$$

Finally, the coupled linear system for pressure and velocity, adding the terms of the Darcy/Forchheimer equation, may be written:

$$\begin{bmatrix} \frac{\mathbf{M}}{\Delta t} + \frac{\mathbf{K}}{Re} + \frac{1}{ReDa}\left(\mathbf{M}_{\varphi} + \mathbf{M}_{\varphi^2} Fo \mathbf{U}\right) & \mathbf{0} & -\mathbf{G}_x \\ \mathbf{0} & \frac{\mathbf{M}}{\Delta t} + \frac{\mathbf{K}}{Re} + \frac{1}{ReDa}\left(\mathbf{M}_{\varphi} + \mathbf{M}_{\varphi^2} Fo \mathbf{U}\right) & -\mathbf{G}_y \\ \mathbf{D}_x & \mathbf{D}_y & \mathbf{0} \end{bmatrix} \begin{bmatrix} u \\ v \\ p \end{bmatrix} = \begin{bmatrix} \frac{\mathbf{M}}{\Delta t} u_d + \frac{\mathbf{M}}{Fr^2} g_x \\ \frac{\mathbf{M}}{\Delta t} v_d + \frac{\mathbf{M}}{Fr^2} g_y \\ \mathbf{0} \end{bmatrix} \tag{17}$$

Here, $\mathbf{U}$ and is the diagonal matrix of the modulus of the velocity at the previous time step in each point of the discrete domain, $\mathbf{M}_{\varphi}$ is the mass matrix considering the ε and φ values of each element, and $\mathbf{M}_{\varphi^2}$, the mass matrix considering an extra φ value of each element, correspondent to the velocity modulus term. Also, $\mathbf{D}_x = \mathbf{G}_x^T$ and $\mathbf{D}_y = \mathbf{G}_y^T$. The temperature is calculated from a separate linear system, as follows:

$$\left[\frac{1}{\Delta t}\mathbf{M}^* + \frac{1}{RePr}\mathbf{K}^*\right]\left[T\right] = \left[\frac{1}{\Delta t}\mathbf{M}^* T_d\right] \tag{18}$$

4. THE SEMI-LAGRANGIAN FORMULATION

After discretizing the spacial derivatives through the finite element method, time derivatives must be discretized as well. Since the material derivative of the velocity results in a non-linear term, a lagrangian approach for that term is used, considering a generic variable ψ, that can either be u, v or T. The semi-lagrangian formulation is, then:

$$\frac{D\psi}{Dt} \approx \frac{\psi - \psi_d}{\Delta t} \tag{19}$$

Where the subscript d denotes the variable's value at the previous time step in the location the fluid particle occupied (x_d) at that time. Figure 2 explicits how the semi-lagrangian method is made and shows an example of mesh used in this method.

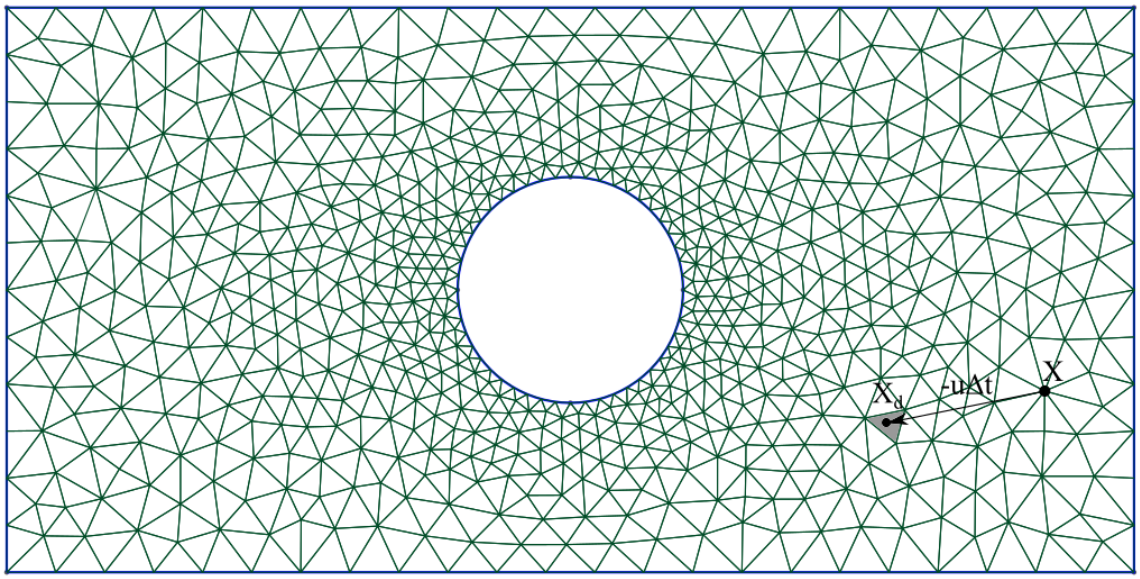

Figure 2: Mesh example and schematic of the semi-lagrangian formulation, where $\mathbf{X}_d$ is the position the fluid particle occupied at the previous time, determined by means of the velocity $\mathbf{u}$ and the time step Δt.

After determining the position $\mathbf{x}_d = \mathbf{x} - \mathbf{u}\Delta t$ of each point in the mesh, including the centroids/midpoints, the variables u_d, v_d and T_d are calculated by means of the interpolation of such variable's value in the points of the element.

5. RESULTS

5.1 The Poiseuille Flow

This common CFD problem consists in a flow between two plane surfaces, as can be seen in Figure 3, for $Re = 100$ and $Fr = 100$. The mesh used has 6170 elements and 11967 nodes. The purpose of this simulation is to verify that the implemented formulation converges to the analytical solution of the Poiseuille flow.

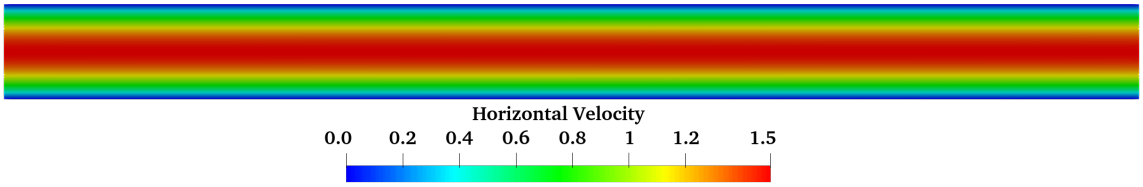

Figure 3: The horizontal velocity field for the Poiseuille flow.

A benchmark comparison was made, in order to verify that the permanent solution converges to the analytical solution. Figure 4 shows said comparison.

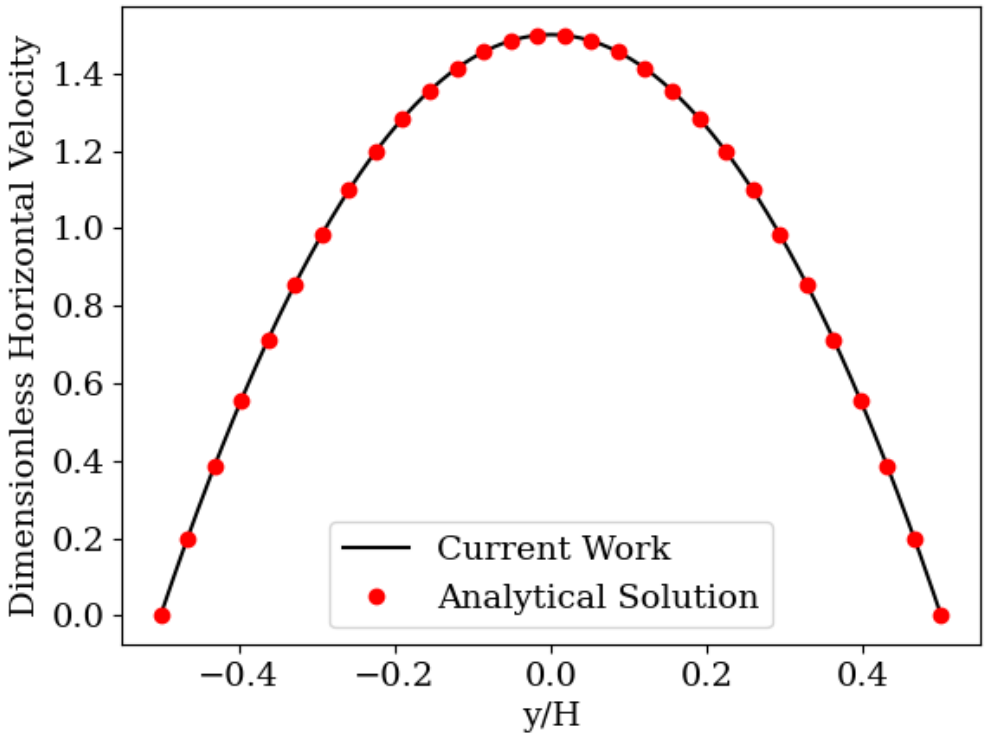

Figure 4: Verification of the Poiseuille Flow through a benchmark comparison.

As can be noticed, both analytical and numerical solutions give the same results, which is a parabola with a maximum value of velocity in the center of the domain.

5.2 The Cavity with Natural Convection

The problem consists in a confined recipient with a temperature difference between the two side walls. In this case, since the characteristic velocity U is not known and there is a temperature gradient ΔT responsible for convective flow, the non-dimensional form of $\mathbf{u}$, t, T and p are given as:

$$\mathbf{u} = \frac{\mathbf{u}_D L}{\nu}, \quad t = \frac{t_D \nu}{L^2}, \quad T = \frac{T_D}{\Delta T}, \quad p = \frac{p_D L^2}{\rho \nu^2} \tag{20}$$

Using equation (20), one may find the non-dimensional form of the continuity and momentum equations for buoyancy dominant effect in a free flow, where T is the temperature, as:

$$\frac{\partial \mathbf{u}}{\partial t} + \mathbf{u} \cdot \nabla \mathbf{u} = -\nabla p + \nabla^2 \mathbf{u} + (Ga - GrT)\mathbf{g} \tag{21}$$

Here $Ga = gL^3/\nu^2$ is the Galileo number and $Gr = gL^3\beta\Delta T/\nu^2$ the Grashof number, with β representing the coefficient of thermal expansion.

Figure 6 shows the stream lines induced by temperature gradient, for $Re = 1$, $Pr = 70.0$, $Ga = 10$ and $Gr = 100$, in a mesh with 1134 elements. The boundary conditions are shown in Figure 5.

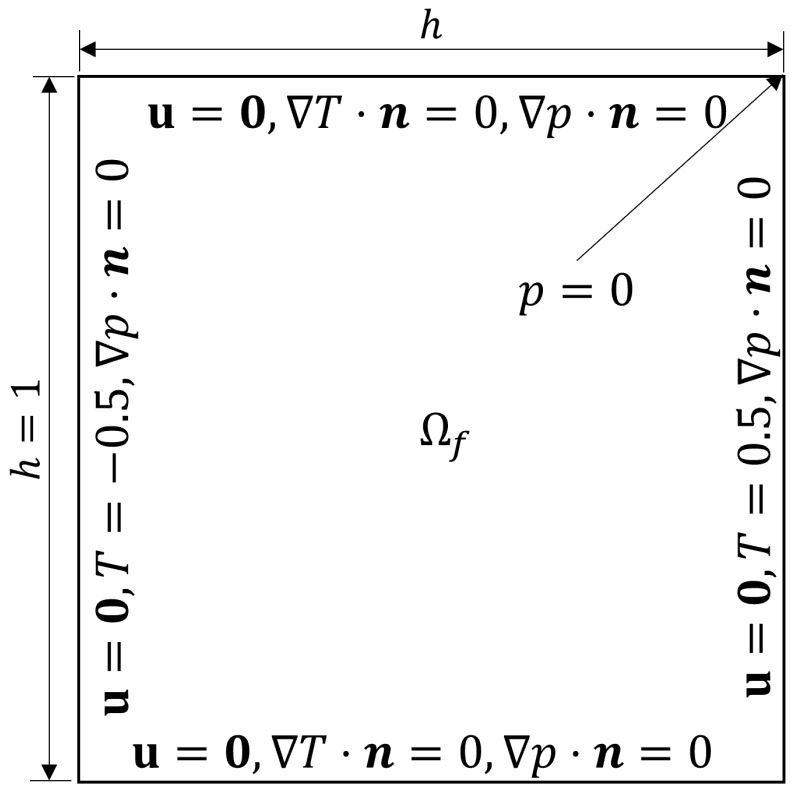

Figure 5: Boundary conditions for the natural convection problem.

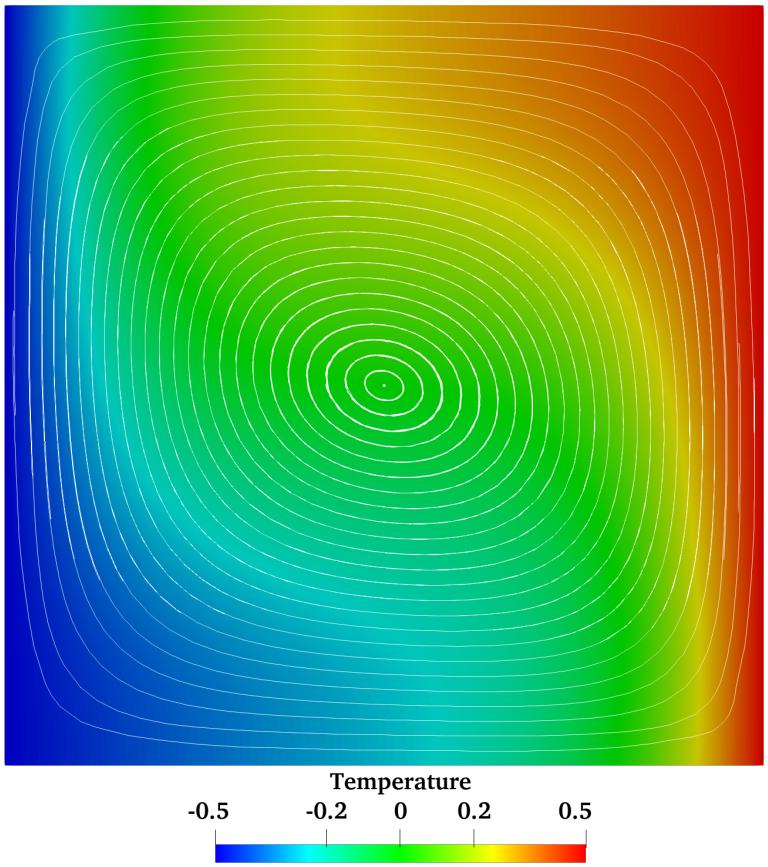

Figure 6: Temperature field with stream lines in the natural convection problem.

The pressure difference between both sides of the cavity provokes convective streamlines, which also interfere in the temperature field, converging to the result observed in Figure 6. Clearly the flow is given in a counter-clockwise direction since the denser part of the fluid is the colder one and it moves in the gravity direction (downwards).

5.3 The Flow over Porous Medium

Finally, the Darcy/Fochheimer model for mixed porous/free media is used to analyze heat transfer and also to validate the model with the Penalization Method proposed by Cimolin and Discacciati (2013). For that, a quadratic element mesh with 9248 triangular elements was used. Figure 7 shows the domain analyzed.

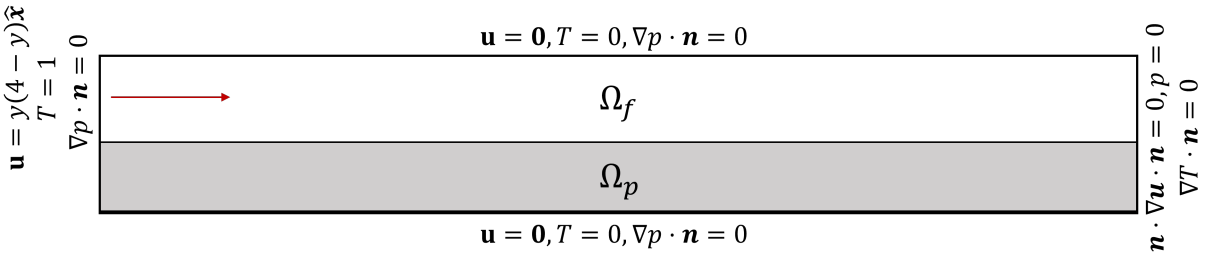

Figure 7: Boundary conditions for the flow over porous medium, for $Re = 6.38$, $Da = 0.373$, $Fo = 1.952$ and $Fr = 100$.

As seen in Figure 7, both upper and lower walls have the no-slip and the impermeability conditions imposed, and so does the backward-facing step. Also, the total length of the channel is 50 and the total height 7, being the horizontal axis located at the interface of the media, located 3 units of length above the bottom interface, so that the Poiseuille condition at the inflow is $u = y(4 - y)$. The simulation for $Re = 6.38$, $Pr = 0.7$, $Da = 0.373$, $Fo = 1.952$ and $Fr = 100$ is presented below, in Figures 8 and 9.

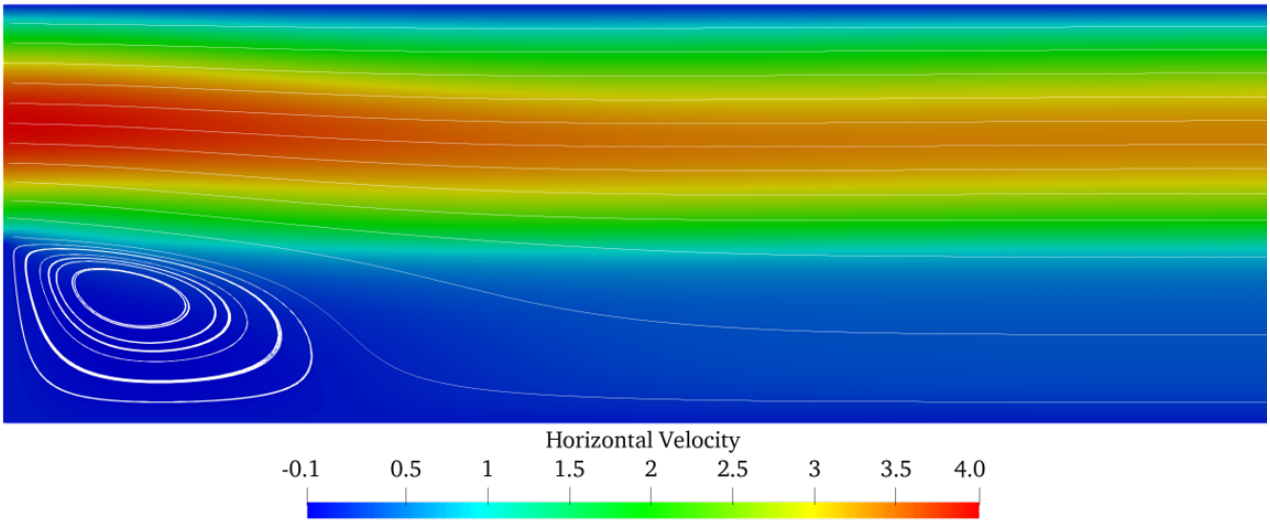

Figure 8: Horizontal velocity field and stream lines for the flow over porous medium, for $Re = 6.38$, $Da = 0.373$, $Fo = 1.952$ and $Fr = 100$.

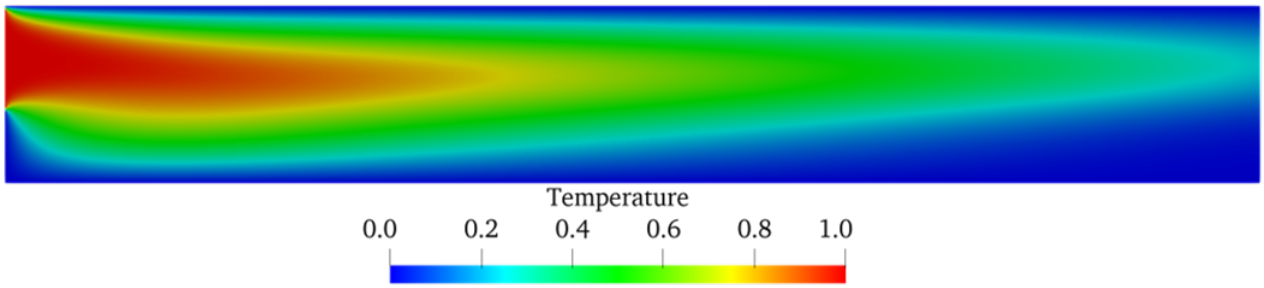

Figure 9: Temperature field for the flow over porous medium, for $Re = 6.38$, $Da = 0.373$, $Fo = 1.952$ and $Fr = 100$.

The velocity field resembles the Poiseuille flow for the Ω_f region due to the high resistance imposed by the porous medium Ω_p.

A recirculation zone is formed near the entry boundary, although with modest values of velocity, since it happens in the porous medium. Along the channel, the flow reaches a fully developed regime, with a velocity field having higher values for the free flow region than for the porous medium, as was expected. Also, the temperature field is highly influenced by convection, as, comparatively, the region that increases the most is the one with a higher average velocity, leaving the porous medium with a lower contribution of convection compared to the free-flow region.

6. CONCLUSION

Throughout this work a literature review on numerical methods for fluid dynamics was presented, including the modeling of the flow in porous medium using the Darcy/Forchheimer equation. Afterwards, the entire math models were presented for mass, momentum and energy balances, considering domains with mixed free and porous regions.

The finite element method is used in the Darcy/Forchheimer differential equation along with continuity and energy ones. For the material derivative, a semi-Lagrangian approach was used, in order to avoid non-linear terms of the equations. The final result is a linear system of equations for which the variables are the pressure, temperature and velocity for each point.

A first validation of the implemented method is made for the traditional lid-driven cavity problem, using a mesh convergence analysis. Then, a convection problem is analyzed with respect to temperature field and streamlines, bringing to discussion the interaction between pressure gradients and velocity fields. Finally, a flow over porous medium was simulated, showing that the porous medium may interfere considerably in the temperature field, since convection is altered when compared to a free-flow in the same domain.

7. REFERENCES

Abdelwahed, M., Chorfi, N. and Hassine, M., 2011. "A stabilized finite element method for stream function vorticity formulation of navier-stokes equations". *Electronic Journal of Differential Equations*, Vol. 2017, No. 24, pp. 1–10.

Bagai, S., Kumar, M. and Patel, A., 2020. "The four-sided lid driven square cavity using stream function-vorticity formulation". *Journal of Applied Mathematics and Computational Mechanics*, pp. 17–30. doi:10.17512/jamcm.2020.2.02.

Batchelor, G.K., 2000. *An Introduction to Fluid Dynamics*. Cambridge University Press, USA.

Bessaih, H., Garrido-Atienza, M.J. and Schmalfuß, B., 2018. "On 3d navier–stokes equations: Regularization and uniqueness by delays". *Physica D*. doi:https://doi.org/10.1016/j.physd.2018.03.004.

Cimolin, F. and Discacciati, M., 2013. "Navier–stokes/forchheimer models for filtration through porous media". *Applied Numerical Mathematics*, Vol. 72, pp. 205–224. doi:https://doi.org/10.1016/j.apnum.2013.07.001.

Mesquida, I.M.V., 2019. *Analysis of Flow Pattern in a Gasoline Particulate Filter using CFD*. Master's thesis, Chemical and Materials Engineering - University of Alberta.

Toro, L., Cardona, C.A., Pisarenko, Y.A. and Frolkova, A.V., 2018. "The finite element method (fem): An application to fluid mechanics and heat transfer". *Fine Chemical Technologies*, Vol. 13, No. 4. doi:10.32362/2410-6593-2018-13-4-17-25.

Zhang, K., Wang, C.A. and Tan, J.Y., 2018. "Numerical study with openfoam on heat conduction problems in heterogeneous media". *International Journal of Heat and Mass Transfer*, pp. 1156–1162.

Zienkiewicz, O.C. and Taylor, R.L., 2000. *The Finite Element Method - Volume 3*. Wiley.

Zitouni, A.H., Spiteri, P., Aissani, M. and Benkheda, Y., 2020. "Thermal and fluid flow modeling of the molten pool behavior during tig welding by stream vorticity method". *International Journal on Interactive Design and Manufacturing (IJIDeM)*. doi:https://doi.org/10.1007/s12008-020-00653-0.

8. RESPONSIBILITY NOTICE

The authors are solely responsible for the printed material included in this paper.